



Robust geotechnical design of braced excavations in clays



C. Hsein Juang^{a,b,*}, Lei Wang^a, Hsii-Sheng Hsieh^c, Sez Atamturktur^a

^a Glenn Department of Civil Engineering, Clemson University, Clemson, SC 29634, USA

^b National Central University, Jhongli City, Taoyuan County 32001, Taiwan, ROC

^c Trinity Foundation Engineering Consultants, Co., Ltd., Taipei, Taiwan, ROC

ARTICLE INFO

Article history:

Available online 6 February 2014

Keywords:

Uncertainty
Probability
Robust design
Optimization
Wall deflection
Braced excavation
Clay

ABSTRACT

In this paper, the authors present a methodology for the robust geotechnical design (RGD) of braced excavations in clayey soils. The maximum wall deflection induced by the excavation was chosen as the response of concern in the design and was computed using a finite element analysis model based upon the beam-on-elastic-foundation theory. The *variation* of the maximum wall deflection of a given design of a braced excavation due to uncertainty in the soil parameters and the surcharges was used as a measure of the design *robustness*. The robust design of the braced excavation system (including soil, wall, and support) was then formulated as a multi-objective optimization problem, in which the variation of the maximum wall deflection (a signal of the design robustness) and the cost were optimized with the strict safety constraints. Using a multi-objective genetic algorithm, the optimal designs were then determined, the results of which were presented as a Pareto Front that exhibited a trade-off relationship useful for design decision-making. Furthermore, the “knee point” concept, based upon the “gain-sacrifice” trade-off is used in the selection of the most-preferred design from the Pareto Front. Finally, a design example of a braced excavation system was used to illustrate the significance of this proposed methodology.

© 2013 Elsevier Ltd. All rights reserved.

1. Introduction

Designing a braced excavation system (i.e., soil–wall–support system) in an urban environment in the face of uncertainty is a risky geotechnical operation, in that the “failure” of such a system (defined as the collapse of the excavation system or exceeding the allowable wall and ground settlement) can have detrimental effects on adjacent structures, with accompanying adverse social and economic effects. One recent excavation failure occurred in Singapore [3] in which a stretch of the Nicoll Highway collapsed after the retaining wall that supported the excavation for a Mass Rapid Transit (MRT) tunnel failed. In this collapse, four lives were lost, damages ran into the millions and the project was delayed for approximately a year.

The deterministic design approach is commonly employed in the traditional design of braced excavations. There are two types of design requirements: the stability of the excavation system itself (known as the *stability* requirement) and the protection of adjacent structures against excavation-induced damage (known as the *serviceability* requirement). Two failure modes must be evaluated when ensuring stability: the basal heave failure and the push-in failure [18]. For the serviceability requirement, the wall and/or ground deformations caused by the excavation must be evaluated

and controlled to prevent damage to the adjacent structures. Thus, the owner or regulatory agency often establishes the limiting factors of safety for stability requirements and the limiting maximum wall and/or ground settlement as a means of preventing damage to adjacent infrastructures, respectively [6,11,18,21,25]. The uncertainties in the soil parameters, however often makes it difficult to determine with *certainty* if both stability and serviceability requirements in a braced excavation are satisfied. As such, the engineer often faces conflicting goals in either overdesigning a structure for greater liability control or under-designing the structure to cut costs. To address this dilemma, the authors present a robust geotechnical design (RGD) framework for purposes of designing braced excavations in clays. This RGD framework is adapted from the very recent work by Juang and his co-workers [12,26] with a significant modification for design of braced excavation systems. The modification is mainly reflected in the way the design robustness is defined and implemented.

Originally proposed by Taguchi [24] for product quality control in manufacturing engineering, the concept of robust design has been used in mechanical and aeronautical designs [1,17,19,22]. Any successful robust design concept must encompass both *easy-to-control* parameters, such as the dimension of a diaphragm wall and layout of struts for braced excavations, and *hard-to-control* factors such as uncertain soil parameters, which are referred to herein as noise factors. In that the uncertainty of these noise factors cannot be fully eliminated, the design objective becomes one

* Corresponding author at: Glenn Department of Civil Engineering, Clemson University, Clemson, SC 29634, USA. Tel.: +1 864 656 3322; fax: +1 864 656 2670.
E-mail address: hsein@clemson.edu (C.H. Juang).

of reducing the effects of the uncertainty of these noise factors on the response of the system. Therefore, the purpose of the robust design method is to derive a design that is robust against the effects of the uncertainty of these noise factors, thereby reducing the variability of the system response.

In this paper, we describe our implementation of a robust geotechnical design (RGD) of braced excavations in a multi-objective optimization framework, within which all possible designs were first screened for *safety* requirements (including, in this paper, stability and serviceability requirements). For the designs that satisfy the safety requirements, the cost and robustness were evaluated, and those designs were then optimized with the two objectives of minimizing the cost and maximizing the robustness. Because the two objectives are often conflicting, as is shown later, the result of the optimization is not a single best design, but rather a set of *non-dominated* designs [4], the collection of which is known as the Pareto Front [2]. The Pareto Front yields a trade-off relationship between the cost of the braced excavation and the robustness of that excavation design, which may be used to select the most preferred design.

2. Deterministic model for evaluating the excavation-induced wall deflection

The maximum wall deflection caused by a braced excavation is often used as a basis for field control to prevent damage to the adjacent infrastructures for two reasons. First, it is generally easier to achieve a greater accuracy in predicting the maximum wall deflection, as opposed to predicting ground settlement [9,13], during the design. Second, it is easier to measure accurately the wall deflection than to measure ground settlement during the construction. Also because the maximum wall deflection is known to correlate with the maximum ground settlement [13,16], we selected the maximum wall deflection as the system response of concern for the robust design of the braced excavation system.

In this study, a computer code TORSAs (Taiwan Originated Retaining Structure Analysis) created by Trinity Foundation Engineering Consultants (TFEC) Co. and based upon the beam-on-elastic foundation theory, was adopted as the deterministic model for predicting the maximum wall deflection. This commercially available code has been validated and widely used by engineers in the design of braced excavations in Taiwan [23]. In the beam-on-elastic foundation approach to simulating soil-structure interaction, the Winkler model is often applied, in which the retaining wall is simulated as a continuous beam of unit width, with the soils treated as springs [18,23]. In TORSAs, the Winkler model is solved with the finite element method (FEM). The selection of TORSAs as our deterministic model in this study is mainly motivated by its proven accuracy in predicting the maximum wall deflection, its execution speed, and the ease with which it is implemented into our robust design framework (to be elucidated later).

For a braced excavation in clay, the system response (i.e., maximum wall deflection) was determined to be the most sensitive to the normalized undrained strength (s_u/σ'_v) and the normalized modulus of horizontal subgrade reaction (k_h/σ'_v) [10,18]. These two parameters are usually quite uncertain due to soil variability and measurement error. Thus, they are treated as “noise factors” in the context of the robust design.

3. Methodology for geotechnical robust design of braced excavations

3.1. Robust design concept and parameters setting

In a typical braced excavation design, the geometric dimensions (length, width, and depth) of the excavation are determined by

either the structural engineer or the architect. For a braced excavation in clay using a diaphragm wall, the length of the wall (L), the thickness of the wall (t), the vertical spacing of the struts (S), and the strut stiffness (EA) are the design parameters. In the context of robust design, these are known as “easy to control” parameters because they are specified by a designer. The soil-related input parameters that exhibit a dominant effect on the maximum wall deflection in a braced excavation are the normalized undrained shear strength (s_u/σ'_v) and the normalized modulus of horizontal subgrade reaction (k_h/σ'_v), as noted previously. Besides, the surcharge behind the diaphragm wall (q_s) was also considered as a noise factor. They are treated as noise factors that exhibit significant variability and are “hard to control” (meaning that it is almost impossible for the designer to remove entirely the uncertainty in these parameters).

The purpose of a robust design, particularly in the case of a braced excavation, is to desensitize the system response of a “satisfactory” design to noise factors. Let us assume a braced excavation design scenario where the system response of concern is the maximum wall deflection (δ_{hm}). The noise factors are s_u/σ'_v , k_h/σ'_v , and q_s , and the design parameters are L , t , S and EA . A design is considered “satisfactory” if it satisfies all the stability requirements (e.g., the computed factor of safety FS_j greater than the specified minimum FS_j) and the serviceability requirement (the computed δ_{hm} value less than the specified allowable value). Within our robust geotechnical design, the goal is to derive a satisfactory design by selecting a proper set of design parameters (L , t , S , EA) so that the system response, in the form of the maximum wall deflection (δ_{hm}), is sufficiently robust to withstand the variation in noise factors (s_u/σ'_v , k_h/σ'_v , q_s).

3.2. Developing a general robust geotechnical design (RGD) procedure

The objective of the proposed RGD approach, an example of which is illustrated with a flowchart as shown in Fig. 1 for a braced excavation, was to identify the most optimal design (or a set of optimal designs) that was not only “satisfactory” (i.e., meeting the safety requirements) but also “robust” and “cost-efficient.” The RGD framework is summarized as follows:

In Step 1, we defined the problem of concern and classified the design parameters and the noise factors for all input parameters of the braced excavation system, as described in the previous section.

In Step 2, we then characterized the uncertainty of noise factors and specified the design domain. For a braced excavation in clay, the noise factors in the context of robust design in this study include s_u/σ'_v , k_h/σ'_v , and q_s . The uncertainty in these noise factors is often quantified using the available data from site investigation and experiences with similar projects.

For the design parameters, the design domain should be defined based upon their typical ranges, augmented with local experiences. These design parameters should be specified in discrete numbers for convenience in construction. Thus, the design domain will consist of a finite number (M) of designs.

In Step 3, we then derived the mean and variance of the system response for robustness evaluation. Recall that a smaller variation (in terms of standard deviation) in the system response indicates a greater robustness. Thus, to assess the robustness of a design, the mean and standard deviation of the system response should be evaluated. In this paper, the Point Estimate Method (PEM; see [8,15]) is used to derive the mean and standard deviation of the system response in conjunction with TORSAs.

Deriving this mean and variance was most challenging in the context of solving a braced excavation problem, as the “performance function” for the excavation-induced response is a finite element model without an *explicit* function. It involved coupling of the PEM-based reliability analysis (implemented through a

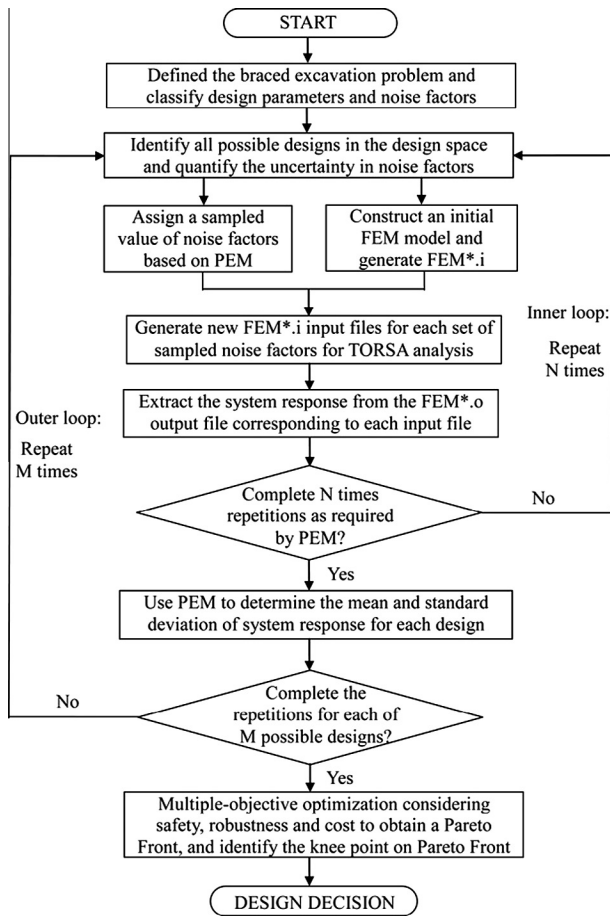


Fig. 1. Flowchart of the proposed robust geotechnical design of braced excavations.

Matlab program) and the deterministic FEM code (TORSAs), as shown in the inner loop in Fig. 1. For a given set of design parameters, the *initial* FEM model (the baseline model that is evaluated with only the mean values of the noise factors) is used, and the model file is written and saved as **FEM*.i** (input file name), which contains all necessary data for a FEM analysis with TORSAs. In this paper, the PEM approach was used to evaluate both mean and standard deviation of the system response. The PEM required evaluating the system response at each of the N sets of the sampling points of the noise factors ($N = 2^n$, where n is the number of input noise factors). In each repetition, the values of noise factors for each set of the PEM sampling points were assigned. The corresponding new **FEM*.i** input file for each of the N set of sampling points was generated by modifying the initial **FEM*.i** input file. The system response for each of the N set of sampling points was obtained by automatically running TORSAs (the FEM code) in the Matlab environment with the corresponding **FEM*.i** input file. The post-processing was undertaken upon completion of the TORSAs solution process, and the system response was extracted from the corresponding **FEM*.o** output file generated from the input file. The resulting N system responses were then used to evaluate the mean and standard deviation of system response based upon the PEM formulation.

In Step 4, we repeated our analysis in Step 3 for each of M designs in the design space. Here, the design parameters in the **FEM*.i** input file were modified automatically in each of the repetitions of Step 3 and the mean and standard deviation of the system response for each design in the design space were determined. This step is represented by the outer loop shown in Fig. 1.

In Step 5, we performed the multi-objective optimization considering the design objectives and design constraints to seek for robust design solutions. The objectives of this robust design scheme involve two distinct criteria: one involves enhancing the robustness, which is accomplished by minimizing the variation in the system response (maximum wall deflection), and the other involves enhancing the economic efficiency by minimizing the cost. The safety requirements, which include the stability and serviceability requirements, are implemented as the design constraints, which can be specified either deterministically or probabilistically.

Note that a unique optimal solution at which all objectives are optimized is highly unlikely for an optimization problem with multiple, and often conflicting, objectives. Rather, a Pareto Front composed of non-dominated solutions (see Fig. 2) is usually obtained. A non-dominated solution is the one in which the improvement of the design in any one objective can only be achieved at expense of the others [12,26]. Fig. 2 shows a possible optimization outcome in a bi-objective space where the Pareto Front lies on the boundary of the feasible region [2]. Thus, the optimal solutions on the Pareto Front are the “best compromise solutions” that are optimal to both objectives. In this paper, the authors used a Non-dominated Sorting Genetic Algorithm version-II (NSGA-II) to obtain these optimal solutions, the procedures of which are detailed in Deb et al. Deb et al. [4]. Using the NSGA-II procedure, a Pareto Front (a set of optimal designs) can be established, which defines a “sacrifice-gain” trade-off relationship between cost and robustness.

If the desired cost/robustness level is specified, the Pareto Front is readily applicable to select the most preferred design. Should there be no available information about the desired level of cost/robustness, a knee point concept (described later) may be used to select the single most preferred design based on the “sacrifice-gain” relationship displayed by the Pareto Front.

4. Estimation of the cost in a braced excavation

Cost-efficiency must be considered in the design of any geotechnical system [27,28]. The total cost of braced excavation includes the costs of the diaphragm wall, costs of the bracing system, costs of excavation/disposal of the dirt, costs of dewatering of the site, and costs of placement of the requisite instrumentation. Because the site dimension and excavation depth is fixed for any

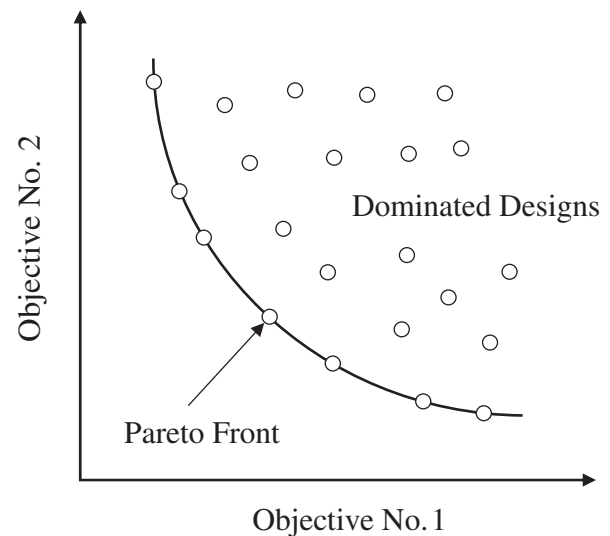


Fig. 2. Illustration of a Pareto Front in a bi-objective space (modified after [2]).

such project, the costs for the last three terms are equal and the major optimization item for the cost of the braced excavation is the cost of the supporting system (including both the diaphragm wall and bracing system). Thus, the total cost for the supporting system Z is the summation of the cost of the diaphragm wall and the bracing system, which is expressed as:

$$Z = Z_w + Z_b \quad (1)$$

where Z_w is the cost of the diaphragm wall; Z_b is the cost of the bracing system.

The cost of the diaphragm wall is proportional to the volume of the wall. As the perimeter length of a specific site is a fixed number, the cost of the diaphragm wall is determined by the length and thickness of wall, which is expressed as:

$$Z_w = c_w \times D \times L \times t \quad (2)$$

where Z_w is the cost of the diaphragm wall; c_w is the unit cost of diaphragm wall per m^3 ; D is the perimeter length of the excavation (m); L is the length of the wall (m); and t is the thickness of the wall (m). The unit cost of diaphragm wall c_w (including both material and labor costs) is approximately NT \$10,000/ m^3 in local practice (i.e., braced excavation in clays in Taipei), which corresponds to approximately 330 USD/ m^3 (assuming that the currency exchange rate between the US Dollar and the New Taiwan Dollar is 1:30, i.e., NT \$1000 \approx USD \$33).

The cost of the bracing system (e.g. struts consisting of H-section steels) is proportional to the total weight of the bracings. The total weight of the bracing, in turn, is proportional to the number of vertical levels of the struts and the area of the excavation, which is expressed as:

$$Z_b = c_b \times A \times k \times n \quad (3)$$

where Z_b is the cost of the bracing system; c_b is the unit cost of the bracing system per m^2 per level; A is the area of the excavation site (m^2); k is the number of struts per level; n is the number of vertical levels of struts in that bracing system. The unit cost of the bracing system c_b (including both material and labor costs) is approximately NT \$1000/ m^3 in local practice, which corresponds to approximately 33 USD/ m^3 . Thus, in sum, the total cost for the supporting system Z is a function of all design parameters. Five strut alterations per level were considered in our design example (presented later) for purposes of determining the strut stiffness: H300, H350, H400, 2@H350 and 2@H400 (note: 2@H350 here means two H350 struts implemented at the same level; likewise, 2@H400 stands for two H400 struts). The cost difference between H300, H350 and H400 was generally negligible since the main cost incurred was that for the installation of the struts themselves, the cost of which is related to the number of struts per level. This expense, in turn, corresponded to the design parameter of the strut stiffness per level.

The cost in a braced excavation for purposes of robust design optimization described previously is based on the extensive experience of TFEC, a specialty design-built engineering firm, for braced excavations in Taiwan using the diaphragm walls. This is used as an example to illustrate the RGD methodology; other suitable cost schemes can be used in conjunction with the proposed RGD methodology.

5. Robust geotechnical design of braced excavation – case study

5.1. Brief summary of the example of braced excavation

To illustrate the proposed RGD method, we used a case study of braced excavation design in clays, with the soil profile at the excavation site a homogenous clay layer with the ground water table

set at 2 m below the ground surface. The clay is assigned a deterministic unit weight of 1.9 ton/ m^3 . The excavation site, the dimensions of which are pre-defined by architectural and structural requirements, is rectangular in shape with a length of 40 m and a width of 25 m. The final excavation depth is 10 m and the diaphragm wall with multiple struts was employed as the retaining structure. There are three uncertain noise factors in the design. The normalized undrained strength (s_u/σ'_v) is assumed to have a mean of 0.32 and a coefficient of variation (COV) of 0.2, and the normalized modulus of horizontal subgrade reaction (k_h/σ'_v), is assumed to have a mean of 48 and a COV of 0.5. These two soil parameters are assumed to be positively correlated with a correlation coefficient of 0.7. The COV values of the two soil parameters and the correlation coefficient between these two soil parameters are estimated based on local experience (Ou, 2013, personal communication) and published literatures [10,14,20]. The surcharge behind the wall is assumed to have a mean of 1 ton/m and a COV of 0.2 [14].

As noted previously, the length (L) and the thickness of the wall (t), the vertical spacing of the struts (S), and the strut stiffness (EA) are the design parameters. In this particular example of braced excavation in a uniform clay layer, the length of the wall L typically ranges from 20 to 30 m with increments of 0.5 m, and the thickness of wall t ranges from 0.5 to 1.3 m with increments of 0.1 m. The strut stiffness EA typically assumes a value from one of the five strut implementations: H300, H350, H400, 2@H350 and 2@H400. As a design routine, the preload of the strut is a fixed number depending upon the type of strut. For example, as in the previous design case in which H300 was assigned a preload of 50 tons, H350 was assigned a preload of 75 tons, and H400 was assigned a preload of 100 tons [23]. For a typical excavation project undertaken in clay soil, the first level of strut is typically set at 1 m below the ground surface, and the last level at 3 m above the bottom of the excavation, with the location of all struts set at approximately 1 m above the excavation depth at that stage, except for the last stage [13,23]. Thus, there are four practical choices in the vertical spacing of the struts S in this case: 1.5, 2, 3 and 6 m, which corresponds to the number of struts (5, 4, 3 and 2 in this case), as shown in the layout of struts in Fig. 3. Based upon the combination of the design parameters (L , t , S , EA), there are totally 3780 possible discrete designs in the design space.

5.2. Optimization of braced excavation to obtain Pareto Front

For each of all the designs in the design space, PEM is used in evaluating both the mean and standard deviation of the maximum wall deflection given the noise factors, and the cost estimation method described previously is used in computing the cost of the supporting system of each design. With all these data, a thorough multi-objective optimization, using NSGA-II, which considers safety, robustness and cost, is then undertaken. In this configuration, the stability and serviceability constraints are enforced to ensure the safety of the braced excavation, and then the standard deviation of wall deflection is minimized to ensure robustness, and the cost-efficiency is achieved by minimizing the costs for the supporting system of the braced excavation. A formulation for the robust design of this braced excavation using NSGA-II is illustrated in Fig. 4.

The population size of 100 with 100 generations (note: these are the limits chosen for optimization) is adopted in the NSGA-II optimization. It is noted that the points on the Pareto Front were initially very scattered, but they gradually converged to the final Pareto Front. The converged results were obtained at 20th generation (or iterations) for this braced excavation design example, which yielded 25 “unique” non-dominated optimal designs. The

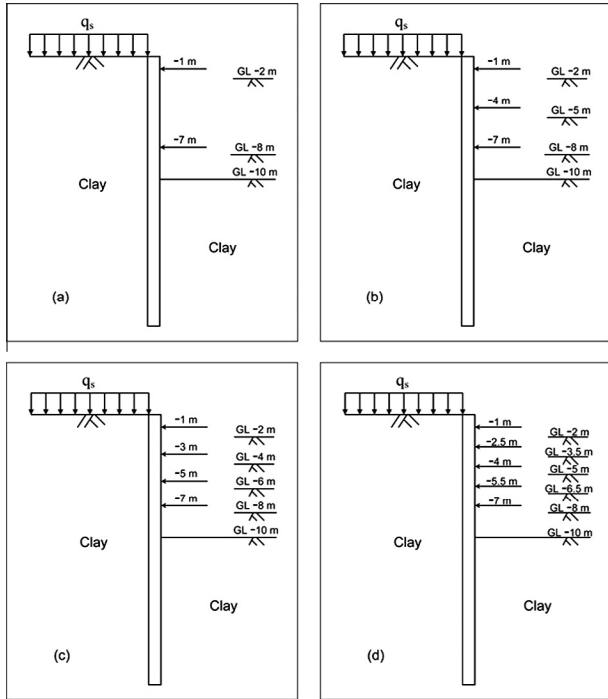


Fig. 3. Four different strut layouts for the design of braced excavations: (a) 6 m spacing; (b) 3 m spacing; (c) 2 m spacing; and (d) 1.5 m spacing.

Given: $L_E = 40$ m (length of excavation)
 $B_E = 25$ m (width of excavation)
 $H_f = 10$ m (final excavation depth)

Find the value of Design Parameters:
 t (wall thickness), L (wall length), S (strut spacing), EA (strut stiffness)

Subject to Constraints:

$t \in \{0.5 \text{ m}, 0.6 \text{ m}, 0.7 \text{ m}, 0.8 \text{ m}, \dots, 1.3 \text{ m}\}$
 $L \in \{20 \text{ m}, 20.5 \text{ m}, 21 \text{ m}, 21.5 \text{ m}, \dots, 30 \text{ m}\}$
 $S \in \{1.5 \text{ m}, 2 \text{ m}, 3 \text{ m}, 6 \text{ m}\}$
 $EA \in \{\text{H300}, \text{H350}, \text{H400}, 2@\text{H350}, 2@\text{H400}\}$
 Mean factor of safety for the push-in and basal heave ≥ 1.5 [17]
 Mean maximum wall deflection ≤ 7 cm ($0.7\%H_f$, [20])

Objective:

Minimizing the standard deviation of the maximum wall deflection (cm)
 Minimizing the cost for the supporting system (USD)

Fig. 4. Formulation of the robust geotechnical design of braced excavations with NSGA-II.

parameters of these designs are listed in Table 1, which collectively constitute the Pareto Front shown in Fig. 5.

The Pareto Front shown in Fig. 5 offers a trade-off relationship between robustness (measured in terms of standard deviation of wall deflection) and cost of the excavation system (or more precisely, the supporting system). Reducing the standard deviation of the wall deflection (and enhancing the robustness) requires an increase in the cost of the supporting system. It should be noted that all designs on Pareto Front are satisfactory with respect to the deterministic safety constraints.

Table 1
List of the designs on the Pareto Front with a deterministic constraint.

No.	t (m)	L (m)	S (m)	EA	Robustness (cm)	Cost ($\times 10^6$ USD)
1	0.5	20	3	H350	3.11	0.53
2	0.5	21	3	H350	3.09	0.55
3	0.5	20	2	H350	2.59	0.56
4	0.5	21	2	H350	2.58	0.58
5	0.5	20	1.5	H400	1.29	0.59
6	0.6	20	2	H400	1.07	0.65
7	0.6	20	1.5	H400	1.02	0.68
8	0.8	20.5	3	H400	1.01	0.80
9	0.8	20	2	H400	0.97	0.82
10	0.8	20	1.5	H400	0.96	0.85
11	1	20.5	6	2@H350	0.84	1.01
12	1	21	6	2@H350	0.83	1.03
13	1.1	20	3	2@H350	0.80	1.14
14	1.1	20.5	3	2@H350	0.79	1.17
15	1.2	20.5	6	2@H350	0.77	1.19
16	1.2	21	6	2@H350	0.75	1.21
17	1.2	20.5	3	2@H350	0.72	1.25
18	1.2	21	3	2@H350	0.71	1.28
19	1.2	21.5	3	2@H350	0.70	1.30
20	1.2	21	2	2@H350	0.69	1.35
21	1.2	21.5	2	2@H350	0.68	1.37
22	1.2	22	2	2@H350	0.67	1.40
23	1.2	21.5	1.5	2@H350	0.66	1.44
24	1.2	22.5	1.5	2@H350	0.65	1.49
25	1.2	24	1.5	2@H350	0.64	1.57

Note: Robustness is evaluated in terms of the standard deviation of the maximum wall deflection; a smaller standard deviation indicates a greater robustness.

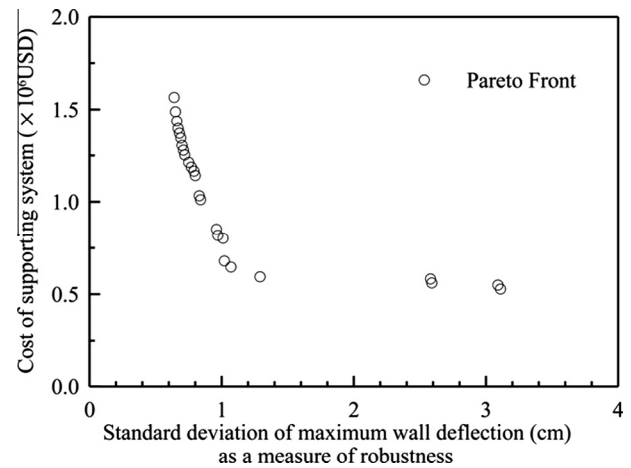


Fig. 5. The Pareto Front optimized for both cost and robustness using deterministic constraints (for robustness, a smaller standard deviation indicates a greater robustness).

By definition, the Pareto-Front includes two groups of designs: (1) of those with an identical level of robustness, the most inexpensive design is selected; (2) of those with an identical level of cost, the most robust design is selected. The decision maker (designer) can then choose a design from this Pareto Front, as any design point is “non-dominated” with respect to these two objectives. Once the designer specifies a cost level, selecting the design with least standard deviation of the wall deflection within the cost level on Pareto Front will provide the most robust design. For example, if the limiting budget for a supporting system is 1×10^6 USD, the design with parameters $t = 0.8$ m, $L = 20$ m, $S = 1.5$ m and $EA = \text{H400}$ is the most robust design (No. 10 design in Table 1) within that cost level. Similarly, the most preferred design may also be selected based on a desired level of robustness. Further discussion of the most preferred design is presented in the section that follows.

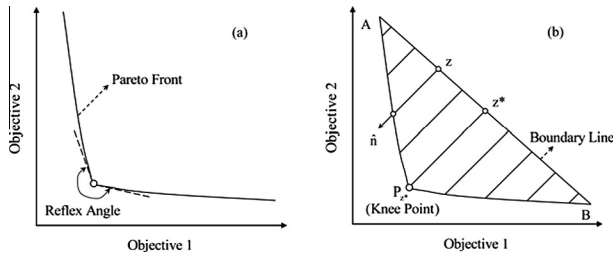


Fig. 6. Illustration of the reflex angle and the knee point identification (modified after [5]).

5.3. Selection of the most preferred design based on concept of knee point

Although the trade-off relationship in terms of a Pareto Front provides valuable information to the designer with which they may make an informed decision by explicitly considering cost and robustness, the designer may prefer to locate a single most optimal design rather than a set of designs. Consequently, additional steps may be necessary to refine this decision-making based upon the Pareto Front for the most preferred solution.

In many cases, in a Pareto Front generated from a bi-objective optimization, there exists a most preferred point, known as the knee point [5]. Any design (i.e., any point on the Pareto Front) apart from the knee point requires a large sacrifice in one objective to achieve a small gain in the other objective. Thus, the knee point may be defined as the point on the Pareto Front that has the maximum reflex angle computed from its neighboring points, as shown in Fig. 6(a). The reflex angle denotes the bend of the point on the Pareto Front from its left to right side, which provides a measure of the gain-sacrifice in the trade-off relationship. The reflex angle is measured from its two neighboring points, however, which is only a local property and may not extend to the entire front. To mitigate this locality issue, Deb et al. [5] used the normal boundary intersection method as illustrated in Fig. 6(b) to further define the knee point. On the Pareto Front in Fig. 6(b), two boundary points, A and B, are used to construct a straight boundary line. For any point on the boundary line z, a corresponding point (Pz) on the Pareto Front along the normal (n) course of the boundary line can be located. The knee point is the point (Pz) on the Pareto Front that has the maximum distance from its corresponding point z* on the boundary line [5].

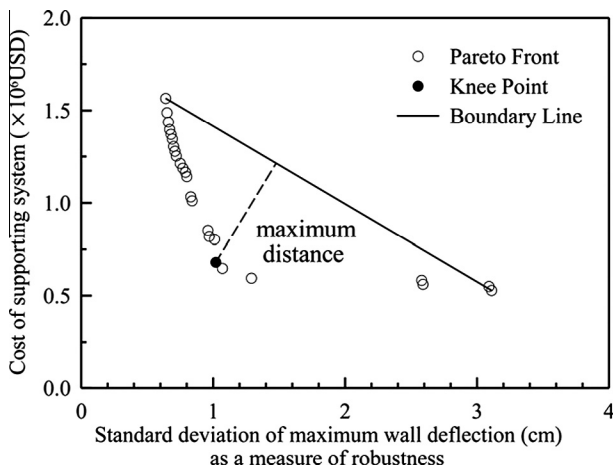


Fig. 7. Example of the knee point identification based upon the Pareto Front in Fig. 5 (for robustness, a smaller standard deviation indicates a greater robustness).

Based upon the definition of the knee point from the concept of the normal boundary intersection method [5], the knee point of the Pareto Front in Fig. 5 is determined by searching for the point farthest from the boundary line. The knee point in Fig. 7 has the following parameters: $t = 0.6$ m, $L = 20$ m, $S = 1.5$ m and $EA = H400$ (No. 7 design in Table 1), with a cost of 0.68×10^6 USD. As shown in Fig. 7, below this cost level, a slight cost increase can significantly improve the robustness (reducing the standard deviation of the wall deflection). Above this cost level (e.g., the cost of the design is further increased sharply), however, the effect of enhancing the robustness (reducing the standard deviation of the wall deflection) becomes markedly inefficient and ineffective.

6. Further discussions

In our analysis described in the previous section, the serviceability requirement of any braced excavation was enforced using a deterministic limiting value. Rather than using a deterministic constraint, the client may prefer to adopt the reliability constraint in terms of the probability of exceedance of a specific limiting value [7,10]. For braced excavation, the serviceability limit state may be defined as:

$$y() = \delta_{hm} - \delta_{lim} \tag{4}$$

where δ_{hm} is the predicted maximum wall deflection (a random variable) and δ_{lim} is the specified limiting maximum wall deflection (usually as a fixed value in the codes). In this paper, for each design in the design domain, the probability of exceedance is computed using Point Estimate Method (PEM) following the procedure documented in Luo et al. [15].

In practice, however, the target probability of exceedance of the specific limiting wall deflection value is not defined explicitly in the design codes and published literatures. Thus, in this section, we describe how to establish Pareto Front using various target levels of probability of exceedance (P_E) as constraints during the optimization process. Through the adoption of various exceedance levels, we can incorporate a degree of flexibility in the robust design process to allow for consideration of allowable risk (i.e., the consequence of the serviceability failure).

For demonstration purposes, the robust design optimization is performed with various reliability constraints, implemented with three levels of probability of exceedance ($P_E < 10\%$, 20% , and 40%). The resulting Pareto Fronts under these constraints are illustrated in Fig. 8, with the detailed design parameters for each design this

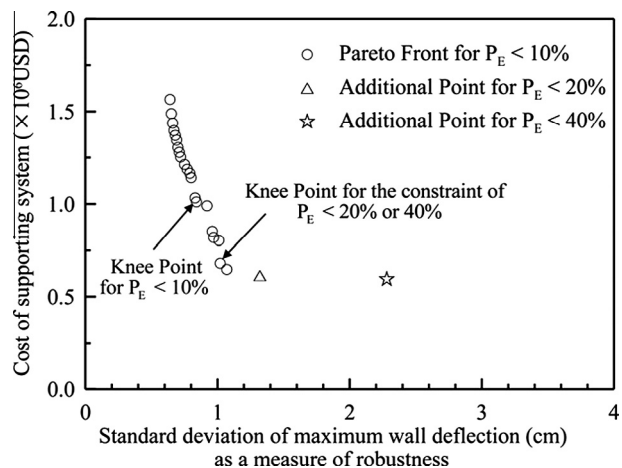


Fig. 8. The optimized Pareto Fronts at various constraint levels of probability of exceedance (for robustness, a smaller standard deviation indicates a greater robustness).

Table 2List of the designs on the Pareto Front with a reliability constraint ($P_E < 40\%$).

No.	t (m)	L (m)	S (m)	EA	Robustness (cm)	Cost ($\times 10^6$ USD)
1	0.5	20	1.5	H350	2.28	0.59
2	0.6	20	3	H400	1.32	0.61
3	0.6	20	2	H400	1.07	0.65
4	0.6	20	1.5	H400	1.02	0.68
5	0.8	20.5	3	H400	1.01	0.80
6	0.8	20	2	H400	0.97	0.82
7	0.8	20	1.5	H400	0.96	0.85
8	1	20	6	2@H350	0.92	0.99
9	1	20.5	6	2@H350	0.84	1.01
10	1	21	6	2@H350	0.83	1.03
11	1.1	20	3	2@H350	0.80	1.14
12	1.1	20.5	3	2@H350	0.79	1.17
13	1.2	20.5	6	2@H350	0.77	1.19
14	1.2	21	6	2@H350	0.75	1.21
15	1.2	20.5	3	2@H350	0.72	1.25
16	1.2	21	3	2@H350	0.71	1.28
17	1.2	21.5	3	2@H350	0.70	1.30
18	1.2	21	2	2@H350	0.69	1.35
19	1.2	21.5	2	2@H350	0.68	1.37
20	1.2	22	2	2@H350	0.67	1.40
21	1.2	21.5	1.5	2@H350	0.66	1.44
22	1.2	22.5	1.5	2@H350	0.65	1.49
23	1.2	24	1.5	2@H350	0.64	1.57

Note: For the constraint of $P_E < 20\%$, all but design No. 1 are on the Pareto Front; for the constraint of $P_E < 10\%$, all but designs No. 1 and No. 2 are on the Pareto Front.

figure listed in Table 2. It is noted that the Pareto Front for the case of $P_E < 20\%$ is almost identical to that for case of $P_E < 10\%$ except that one additional point is identified (No. 2 design in Table 2). Similarly, the Pareto Front for the case of $P_E < 40\%$ happens to generate also one additional point (No. 1 design in Table 2).

Based on the procedure described previously, the knee points obtained for the Pareto Fronts with the constraints of $P_E < 20\%$ and $P_E < 40\%$ are identical. This knee point is a design represented by the following design parameters: $t = 0.6$ m, $L = 20$ m, $S = 1.5$ m and $EA = H400$ (No. 4 design in Table 2), which costs 0.68×10^6 USD. It is interesting to note that this knee point is identical to the knee point obtained previously using the deterministic constraint. If the constrain of $P_E < 10\%$ is adopted, a different knee point is obtained, which has the following design parameters: $t = 1.0$ m, $L = 20.5$ m, $S = 6$ m and $EA = 2@H350$ (No. 9 design in Table 2) with a cost of 1.01×10^6 USD.

The above analysis is based on a limiting wall deflection specified in a Chinese code [21] for a Level III protection of adjacent infrastructures. However, the entire robust geotechnical design (RGD) methodology is easily adaptable for other desired limiting wall deflection requirements.

Finally, it should be noted that unlike the prior work on robust design by Juang and his co-workers [12,26], in which the design robustness was defined through the variation of the failure probability, in the present study the design robustness was defined through the variation of the system response. Here, the standard deviation of the maximum wall deflection is used as the measure of the design robustness. Although further study to select the most appropriate measure (or definition) of the design robustness is desirable, the use of the standard deviation of the maximum wall deflection as the measure of the design robustness is shown effective in the robust design of braced excavation systems in clays.

7. Concluding remarks

In this paper, the authors described a robust geotechnical design (RGD) methodology for addressing the design uncertainties inherent in braced excavations (particularly the uncertainties of geotechnical parameters and surcharges). In the robust design sys-

tem, the purpose is to minimize the effects of these uncertainties through the careful adjustment of the design parameters. Within the robust geotechnical design framework, a multi-objective optimization procedure is used to select designs that are optimal in terms of both cost and robustness, while satisfying all requisite safety requirements. These safety requirements can either be enforced deterministically or probabilistically. As a result, a set of optimal, non-dominated designs, collectively known as Pareto Front, can be obtained. Together with use of a knee point concept, a single most preferred design may be obtained. The established Pareto Front, along with its corresponding knee point, has proven as an effective tool for robust design of braced excavations.

Acknowledgments

The study on which this paper is based was supported in part by National Science Foundation through Grant CMMI-1200117 (“Transforming Robust Design Concept into a Novel Geotechnical Design Tool”) and the Glenn Department of Civil Engineering, Clemson University. The results and opinions expressed in this paper do not necessarily reflect the views and policies of the National Science Foundation.

References

- [1] Chen W, Allen JK, Mistree F, Tsui KL. A procedure for robust design: minimizing variations caused by noise factors and control factors. *J Mech Des* 1996;118(4):478–85.
- [2] Cheng F, Li D. Multiobjective optimization design with Pareto Genetic Algorithm. *J Struct Eng* 1997;123(9):1252–61.
- [3] Committee of Inquiry. Report of the Committee of Inquiry into the Incident at the MRT Circle Line Worksite that led to the collapse of the Nicoll Highway on 20 April 2004. Ministry of Manpower, Singapore; 11 May 2005.
- [4] Deb K, Pratap A, Agarwal S, Meyarivan T. A fast and elitist multiobjective genetic algorithm: NSGA-II. *IEEE Trans Evol Comput* 2002;6(2):182–97.
- [5] Deb K, Gupta S. Understanding knee points in bicriteria problems and their implications as preferred solution principles. *Eng Optim* 2011;43(11):1175–204.
- [6] Finno RJ, Voss FT, Rossow E, Blackburn JT. Evaluating damage potential in buildings affected by excavations. *J Geotech Geoenviron Eng* 2005;131(10):1199–210.
- [7] Goh ATC, Kulhawy FH. Reliability assessment of serviceability performance of braced retaining walls using a neural network approach. *Int J Numer Anal Methods Geomech* 2005;29(6):627–42.
- [8] Harr ME. Reliability-based design in civil engineering. New York: McGraw-Hill; 1987.
- [9] Hashash YMA, Whittle AJ. Ground movement prediction for deep excavations in soft clay. *J Geotech Eng* 1996;122(6):474–86.
- [10] Hsiao ECL, Schuster M, Juang CH, Kung TC. Reliability analysis of excavation induced ground settlement for building serviceability evaluation. *J Geotech Geoenviron Eng* 2008;134(10):1448–58.
- [11] JSA. Guidelines of design and construction of deep excavations. Tokyo, Japan: Japanese Society of Architecture; 1988.
- [12] Juang CH, Wang L. Reliability-based robust geotechnical design of spread foundations using multi-objective genetic algorithm. *Comp Geotech* 2013;48:96–106.
- [13] Kung GTC, Juang CH, Hsiao ECL, Hashash YMA. A simplified model for wall deflection and ground surface settlement caused by braced excavation in clays. *J Geotech Geoenviron Eng* 2007;133(6):731–47.
- [14] Luo Z, Atamturktur S, Cai Y, Juang CH. Simplified approach for reliability-based design against basal-heave failure in braced excavations considering spatial effect. *J Geotech Geoenviron Eng* 2012;138(4):441–50.
- [15] Luo Z, Atamturktur S, Juang CH. Bootstrapping for characterizing the effect of uncertainty in sample statistics for braced excavations. *J Geotech Geoenviron Eng* 2013;139(1):13–23.
- [16] Mana AI, Clough GW. Prediction of movements for braced cuts in clay. *J Geotech Eng Div* 1981;107(6):759–77.
- [17] Marano GC, Sgobba S, Greco R, Mezzina M. Robust optimum design of tuned mass dampers devices in random vibrations mitigation. *J Sound Vibration* 2008;313(3–5):472–92.
- [18] Ou CY. Deep excavation – theory and practice. England: Taylor and Francis; 2006.
- [19] Paiva RM. A robust and reliability-based optimization framework for conceptual aircraft wing design [Ph.D. Thesis]. Canada: University of Victoria; 2010.
- [20] Phoon KK, Kulhawy FH, Grigoriu MD. Reliability based design of foundations for transmission line structures. Rep. TR-105000. Palo Alto, California: Electric Power Research Institute; 1995.

- [21] PSCG. Specification for excavation in Shanghai Metro Construction. Shanghai, China: Professional Standards Compilation Group; 2000.
- [22] Seepersad CC, Allen JK, McDowell DL, Mistree F. Robust design of cellular materials with topological and dimensional imperfections. *J Mech Des* 2006;128(6):1285–97.
- [23] Sino-Geotechnics. User manual of Taiwan originated retaining structure analysis for deep excavation. Taipei, Taiwan: Sino-Geotechnics Research and Development Foundation; 2010.
- [24] Taguchi G. Introduction to quality engineering: designing quality into products and processes. New York: Quality Resources; 1986.
- [25] TGS. Design specifications for the foundation of buildings. Taipei, Taiwan: Taiwan Geotechnical Society; 2001.
- [26] Wang L, Hwang JH, Juang CH, Atamturktur S. Reliability-based design of rock slopes – a new perspective on design robustness. *Eng Geol* 2013;154:56–63.
- [27] Wang Y, Kulhawy FH. Economic design optimization of foundations. *J Geotech Geoenviron Eng* 2008;134(8):1097–105.
- [28] Zhang J, Zhang LM, Tang WH. Reliability-based optimization of geotechnical systems. *J Geotech Geoenviron Eng* 2011;137(12):1211–21.